folded, disconnected, transparent, or opaque, among others. For example, what gives transparency its characteristic appearance, identifiable even from opaque patches in a stereogram (Figs. 2 and 6)?

Because we have no specific data to address this issue directly, we can only speculate. Consider the various distinctive properties of images that are related to surface transparency. This would include, say, stereoscopic T-junction, contrast relations that satisfy Metelli's rule (*28*), simultaneous depth coding from a front and a back plane (*22*), and semispecular reflection at the surface. Given the associative power of theoretical neural networks (*29*), we hypothesize that, if these properties occur simultaneously when the observer locomotes in front of a transparent surface, an associative linkage is formed across these features. Then later, when an image contains a subset of these co-occurring features, the visual system can recall the whole pattern of features. This is presumably why we see transparency in our stereograms even though no transparency exists in the literal sense. Most important for our present discussion, it provides a plausible cluster of neural connections to represent a surface that can then be associated with specific image classes sampled (*30*, *31*).

REFERENCES AND NOTES

1. B. Julesz, *Bell Syst. Tech. J.* **39**, 1125 (1960).
2. H. B. Barlow, C. Blakemore, J. D. Pettigrew, *J. Physiol. (London)* **193**, 327 (1967); G. F. Poggio and B. Fischer, *J. Neurophysiol.* **40**, 1392 (1977).
3. H. Helmholtz, *Handbuch der Physiologischen Optik* (Verlag, Hamburg, 1910) [J. P. C. Southall, Ed. *Helmholtz's Treatise on Physiological Optics* (Dover, New York, 1962)].
4. J. Hochberg, in *Perceptual Organization*, M. Kubovy and J. R. Pomerantz, Eds. (Erlbaum, Hillsdale, NJ, 1981), p. 255; R. L. Gregory, *The Intelligent Eye* (McGraw-Hill, New York, 1970); I. Rock, *The Logic of Perception* (MIT Press, Cambridge, MA, 1983).
5. Related demonstrations indicating the importance of surface representation have been summarized by V. S. Ramachandran, [*Percept. Psychophys.* **39**, 3361 (1986)]; see also V. S. Ramachandran and P. Cavanagh [*Nature* **317**, 527 (1985)].
6. B. Julesz, *Foundations of Cyclopean Perception* (Univ. of Chicago Press, Chicago, 1971).
7. G. F. Poggio and T. Poggio, *Annu. Rev. Neurosci.* **7**, 379 (1984).
8. D. G. Jones and J. Malik, *J. Invest. Ophthalmol. Vision Sci.* **31** (suppl.) 529 (1990).
9. K. Nakayama and S. Shimojo, *Cold Spring Harbor Symp. Quant. Biol.* **40**, 911 (1990).
10. In sparsely textured random dot stereograms, perceived depth of the surface region between dots appears as smoothly interpolated between individual dots (*6*).
11. The technical terms "crossed" and "uncrossed" disparity refer to those disparities that would lead to perceived near and far distances, respectively.
12. S. Shimojo and K. Nakayama, *Perception* **19**, 285 (1990).
13. H. F. J. van Tuijl, *Acta Psychol.* **39**, 441 (1975); C. Redies and L. Spillmann, *Perception* **10**, 667 (1981).
14. W. H. Ittelson, *Visual Space Perception* (Springer, New York, 1960).
15. T. Poggio *et. al.*, *Nature* **317**, 314 (1985).
16. J. J. Gibson, *Perception of the Visual World* (Houghton Mifflin, Boston, 1950); *The Senses Considered as Perceptual Systems* (Houghton Mifflin, Boston, 1966).
17. J. J. Koenderink and A. J. van Doorn, *Biol. Cybern.* **24**, 51 (1976).
18. Although the terms "generic" and "accidental" have been borrowed from the mathematics literature, the terms' exact meanings here and in computer vision have strayed from the precise mathematical definition originally assumed. In our usage, we consider an image I_1 more generic than the other image I_2 when the volume or area in space in which the vantage point can randomly move without causing qualitative change in the image is larger (*17*).
19. The observer should also be relatively far from the display, such that it is effectively a plane parallel projection, otherwise the horizontal limbs will not be collinear because of perspective. Furthermore, the head must not be tilted.
20. J. Malik, *Int. J. Comput. Vision* 1, 73 (1987).
21. I. Biederman, *Comput. Vision Graphics Image Process.* **32**, 29 (1985). See also W. Richards, J. J. Koenderink, D. Hoffman, *J. Opt. Soc. Am. A* **4**, 1168 (1987).
22. K. Nakayama, S. Shimojo, V. S. Ramachandran, *Perception* **19**, 497 (1990).
23. A. Guzman, in *Automatic Interpretation and Classification of Images* A. Grasselli, Ed. (Academic Press, New York, 1969), pp. 243–276; D. A. Huffman, in *Machine Intelligence*, B. Metzler and D. Michie, Eds. (Edinburgh Univ. Press, Edinburgh, Scotland, ed. 6, 1971), pp. 295–323.
24. G. Kanisza, *Organization in Vision: Essays on Gestalt Perception* (Praeger, New York, 1979).
25. D. Marr, *Vision* (Freeman, San Francisco, 1980).
26. The neglect of prior probabilities may be related to recent findings in animal conditioning [R. Rescorla and P. C. Holland, *Annu. Rev. Psychol.* **33**, 265 (1982)]. These studies show that it is not simple contiguity between events that forms associations, but rather that the conditioned stimulus (CS) and unconditioned stimulus (US) must be correlated such that the CS provides unique predictive information about the US. Thus, sheer frequency of pairing alone is not a sufficient precondition for learning. This suggests that, if the frequency of transparent surfaces were extremely rare, these properties of association would enable the generic view of a transparent surface to call forth the perception of transparency even though the number of pairings of an accidental view and an opaque surface was actually more frequent.
27. Our neglect of prior probabilities should also be contrasted to the very different approach taken by H. B. Barlow [*Vision Res.* **30**, 1561 (1990)], where prior probabilities are explicitly registered by changes in neural connection strengths.
28. F. Metelli, *Sci. Am.* **230**, 90 (April, 1974).
29. J. Anderson, *Math. Biosci.* **14**, 197 (1972); T. Kohonen, *IEEE* **C-21**, 353 (1972).
30. In a similar vein, we have previously proposed the importance of associative learning for the perception of subjective contours and surfaces arising from binocularly unpaired image points. The same principle of generic image sampling can apply to these varieties of surface phenomena [K. Nakayama and S. Shimojo, *Vision Res.* **30**, 1811 (1990)].

31. This research was supported in part by grant 83-0320 from the Air Force Office of Scientific Research. S.S. was supported by the Ministry of Education, Sciences, and Culture, Japan.

Detection of Hydrothermal Precursors to Large Northern California Earthquakes

Paul G. Silver and Nathalie J. Valette-Silver

During the period 1973 to 1991 the interval between eruptions from a periodic geyser in Northern California exhibited precursory variations 1 to 3 days before the three largest earthquakes within a 250-kilometer radius of the geyser. These include the magnitude 7.1 Loma Prieta earthquake of 18 October 1989 for which a similar preseismic signal was recorded by a strainmeter located halfway between the geyser and the earthquake. These data show that at least some earthquakes possess observable precursors, one of the prerequisites for successful earthquake prediction. All three earthquakes were further than 130 kilometers from the geyser, suggesting that precursors might be more easily found around rather than within the ultimate rupture zone of large California earthquakes.

One of the basic questions in seismology is whether earthquakes have an observable preparation phase, known as a precursor. This issue is not only central to our understanding of the earthquake process but it is also a prerequisite for successful earthquake prediction. One important approach to this problem is the measurement of crustal deformation: in the far field (more than a few fault lengths away) by long-period seismometers (*1*, *2*) and in the near field by strainmeters (*3*–*5*). In order to observe precursory signals with durations longer than about an hour, however, measurements must be made in the near field, because such signals will not radiate as seismic waves. This major advantage to near-field observations is partially offset by the requirement that the instruments must be near the impending earthquake. This means, paradoxically, that the location of a future earthquake

The authors are at the Department of Terrestrial Magnetism, Carnegie Institution of Washington, 5241 Broad Branch Road, NW, Washington, DC 20015. Part of this work was done while N. J. Valette-Silver was at the Department of Chemistry and Biochemistry, University of Maryland, College Park, MD 20741.

must be predicted before observations relevant to detecting precursors can be made. One way out of this difficulty is to examine a variety of "accidental" strain indicators that can be monitored inexpensively over a large area, such as the hydrologic variations that often accompany tectonic strain. A wide variety of phenomena have been reported (*6*, *7*). In recognition of the important role of hydrologic phenomena, the water levels in wells are presently being monitored in many seismogenic regions of the world and have been carefully calibrated to known sources of crustal deformation such as tidal strain. These observations are an integral part of earthquake monitoring programs in the United States, China, and the former Soviet Union.

Less commonly utilized are hydrothermal phenomena, such as temporal variations in geothermal wells (*8*) or changes in the interval between eruptions (IBE) of periodic or "old-faithful-type" geysers. The sensitivity of the IBE of geysers to the occurrence of earthquakes is, nevertheless, well known. For example, Old Faithful Geyser in Yellowstone, which has been monitored for more than four decades, has shown an increase in IBE after three large earthquakes, including the Borah Peak earthquake of 28 October 1983 (surface wave magnitude M_S = 7.3), particularly noteworthy because of its great distance (240 km) from the geyser (*9*, *10*). The possible presence of precursory variations has also been suggested (*11*). In this article, we analyze nearly 20 years of IBE data for Old Faithful Geyser of California (Calistoga, California, referred to henceforth as Calistoga Geyser) and show that the geyser has exhibited short-term (1 to 3 days) precursory variations in IBE preceding the three largest earthquakes within a 250-km radius of the geyser.

Calistoga Geyser is located (Fig. 1) in an area known for its abundant geothermal activity and studied by scientists for more than 65 years (*12*). In December 1989, while we were visiting the geyser, the existence of several years of IBE data was brought to our attention by Olga Kolbek, manager of the geyser and the geyser monitoring program. She noticed that the IBE data appeared to exhibit a response to the occurrence of certain earthquakes and thought that the geyser might be a useful tool for earthquake monitoring. She kindly made the data available to us.

Description of Seismicity and IBE Data

Several clusters of earthquakes have occurred in the area around the geyser (Fig. 1). To the south of Calistoga have occurred events along the northern end of the San Andreas fault system; to the north, those associated with the Mammoth Lakes region; and to the northeast in the Sierra foothills, the Oroville earthquake of 1 August 1975 (plus two large aftershocks not shown). An examination of seismic activity as a function of moment-magnitude (M_w) and distance from

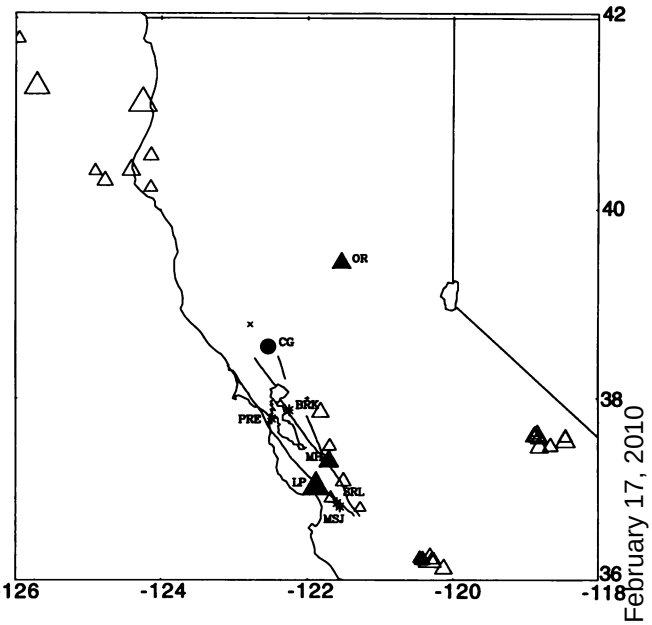

Fig. 1. Location of Old Faithful Geyser of California (Calistoga, California), referred to here as Calistoga Geyser (filled circle, CG). Also shown (triangles) are all earthquakes greater than M = 5.3 that occurred during the period 1973 to 1991 [from the National Earthquake Information Center (NEIC) catalog of the U.S. Geological Survey]. If available, surface wave magnitude M_S was used; if not, body-wave, M_b, or local, M_L, magnitude for smaller events. M_w (based on seismic moment M_0) was occasionally used for larger events if there was a large discrepancy between M_w and M_S. Size of the symbol is proportional to magnitude. Filled triangles denote the three largest events over this time period within a 250-km radius of the geyser. These are LP, the Loma Prieta earthquake of 18 October 1989 [M_0 = 2.5 × 10^{19} N-m, M_w = 6.9 (*14*)]; OR, the Oroville earthquake of 1 August 1975 [M_0 = 1.8 × 10^{18} N-m; M_w = 6.1 (*13*)]; and MH, the Morgan Hill earthquake of 24 April 1984 (M_0 = 2.1 × 10^{18} N-m, M_w = 6.2). Lines south of the geyser denote the major faults: from west to east: the San Andreas fault, the Hayward fault, and the Calavaras fault. Just west and east of the geyser are the Rodgers Creek and West Napa faults (probably extensions of the Hayward and Calavaras faults). Asterisks indicate locations of four strainmeter installations operating during the Loma Prieta earthquake: PRE, BRK, SRL, and MSJ. The location of The Geysers geothermal field is denoted by an x (just north of Calistoga Geyser).

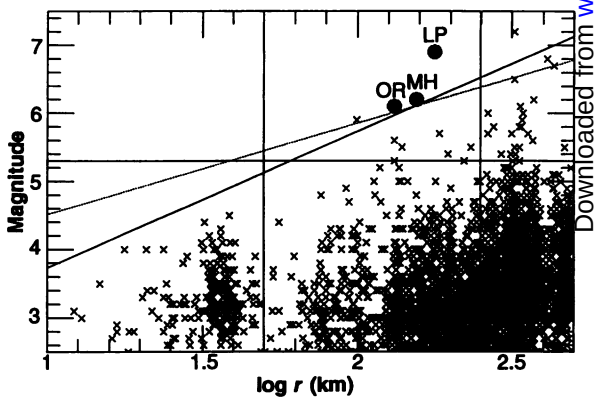

Fig. 2. Plot of seismicity from the NEIC catalog as a function of distance r (<500 km) from the geyser and magnitude M (>2.5). Filled symbols denote the three large events studied. Also shown are vertical lines r = 50 km and r = 250 km, horizontal line giving magnitude cutoff (5.3) in Fig. 1, and two inclined lines that approximately correspond to constant static (solid line, proportional to r^{-3}) and dynamic (dashed line, proportional to r^{-2}) strain at the geyser.

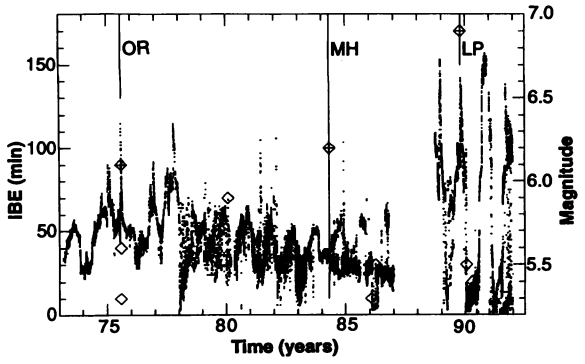

Fig. 3. The entire geyser IBE data set. Each point corresponds to an interval between eruptions. The data have been passed through a median filter (*15*) to enhance coherent features. Also shown are times and magnitudes of all events above M = 5.3 within 250 km of the geyser (diamonds). The times of the three largest events are denoted by vertical lines and crossed diamonds. Data were unavailable for 1987 (lost) and most of 1988 (because of vandalism at the geyser).

the geyser (Fig. 2) provides a means of determining which events should have the greatest effect on the geyser. Among the largest events, in terms of either M_w or calculated strain at the geyser, are the Oroville earthquake [r = 132 km, seismic moment M_o = 1.8×10^{18} N-m; M_w = 6.1 (*13*)], the Loma Prieta earthquake of 18 October 1989 [r = 177 km, $M_o = 2.5 \times 10^{19}$ N-m, M_w = 6.9 (*14*)], and the Morgan Hill earthquake of 24 April 1984 (r = 154 km, $M_o = 2.1 \times 10^{18}$ N-m, M_w = 6.2). We focus on these events.

The eruption times at Calistoga Geyser were recorded in two ways. From 1973 to 1979, they were obtained manually, to the nearest minute for about 10 hours each day during working hours. Since 1980, eruption times have been recorded automatically and continuously by an infrared sensor to the nearest minute for 1980, 1981, 1982, and 1990, and to the nearest second for the other years. After the data had been carefully checked for timing errors, they were converted into an IBE time series (Fig. 3) (*15*). There are several well-defined peaks in the IBE data, and the Oroville and Loma Prieta earthquakes are coincident with two of them. In addition, for certain periods of time the IBE has a multimodal (more than one dominant eruption interval) pattern rather than a unimodal (one predominant eruption interval) pattern. The cause of this multimodality is not entirely clear, but it is a common feature of other geysers, such as Old Faithful Geyser in Yellowstone (*16–18*). The time of the Morgan Hill event appears to mark a change from unimodal to multimodal behavior.

For these three large earthquakes, we plotted the IBE records for 1 year of data (Fig. 4, A to C) and for 50 days of data centered around the origin times (Fig. 4, D to F). The times of the Loma Prieta and Oroville events correspond to the largest interval-lengthening events within their respective years. In the case of Loma Prieta (Fig. 4A) the IBE increased from 90 to 150 min and then returned to the pre-earthquake value after about 70 days. Similarly,

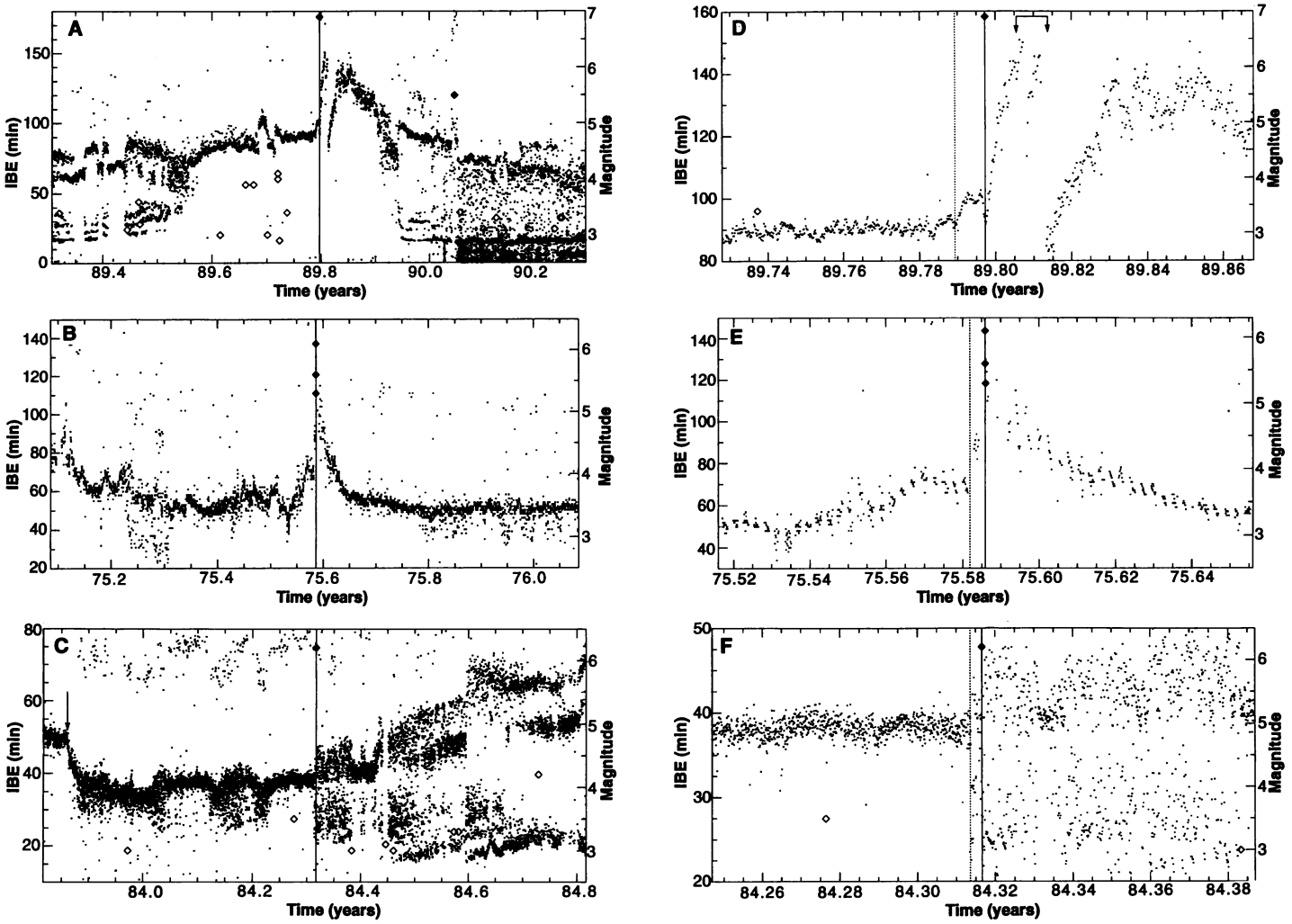

Fig. 4. (**A**) One year of raw data (no filter) centered around the time of the Loma Prieta earthquake (vertical line). Also shown are all earthquakes within a 50-km radius of the geyser (open diamonds) and those earthquakes above M = 5.3 within 250 km of the geyser (crossed diamonds). The earthquake is coincident with the largest episode of interval lengthening of the year. IBE returned to pre-earthquake levels after ~70 days. A smaller interval-lengthening event at 1989.7 may be associated with the cluster of four events ($M \sim 4$) near The Geysers geothermal field (Fig. 1). (**B**) Same as (A) except for the Oroville earthquake (diamonds denote the main event and two aftershocks). Event time is coincident with the largest episode of interval lengthening of the year. IBE returned to pre-earthquake levels after ~40 days. (**C**) Same as (A) except for the Morgan Hill earthquake. Earthquake time is coincident with a change from a unimodal to a multimodal pattern of eruptions. The abrupt drop in IBE near 1983.9 is coincident with the largest daily precipitation of the year of 9 cm (arrow), suggesting that the decrease was rain-induced. (**D**) Fifty days of raw IBE data centered on the Loma Prieta earthquake. Interval lengthening began ~60 hours (0.0068 year) before the event (dashed line). Rapid drops in IBE after the earthquake are coincident with the largest 4-day period of precipitation of the year (arrows), suggesting that they are rain-related. (**E**) Same as (D) except for the Oroville earthquake. Interval lengthening begins about a day before the event (dashed line). (**F**) Same as (D) except for the Morgan Hill earthquake. The change from unimodal to multimodal behavior occurred ~1 day before the earthquake.

for Oroville (Fig. 4B), the IBE increased from 50 to 120 min and returned to a value of 50 min after about 40 days. In the case of the Morgan Hill event, the IBE (Fig. 4C) changed from a unimodal (IBE ~40 min), to trimodal (IBE ~25, 40, and 50 min) pattern close to the event time, which then persisted for at least the next 6 months.

The more detailed plots (Fig. 4, D through F) demonstrate the remarkable correspondence between event time and IBE behavior and show that IBE variations began before the earthquakes occurred. Before the Loma Prieta event, the IBE fluctuated around a value close to 90 min. Within 4 days, it rapidly doubled. Close examination reveals that the interval lengthening began at least 60 hours before the event and reached a preseismic value of about 100 min, well above the baseline defined by the previous month of data. The event time is seen as a local minimum between the preseismic and coseismic changes. Similarly, for the Oroville event, the IBE doubling began a day before the earthquake, where there is a cluster of points (IBE ~80 to 90 min) significantly above the baseline for the previous month. Finally, the change from a unimodal pattern to a highly scattered trimodal pattern occurred about a day before the Morgan Hill earthquake.

We studied in detail the time period corresponding to every other earthquake above magnitude 5.2 at a radius between 200 and 500 km, above magnitude 5.0 within a radius of 200 km, and above magnitude 3.5 for a radius less than 50 km. None of these earthquakes is coincident (within 1 to 2 days) with a change in IBE that is near the clarity of the three events in Fig. 4. The closest are the cluster of four relatively large local events (M ~ 4) that occurred in August and September 1989 (Fig. 4A) about 40 km northwest of the geyser near "The Geysers" geothermal field (Fig. 1). Finally, none of these other events appear to be correlated with either the preseismic or the coseismic variations that we have associated with the three major earthquakes seen in Fig. 4.

Influence of Other Physical Factors

Other physical phenomena, such as precipitation, changes in barometric pressure, and local hydrological variations, might perturb the IBE. These factors must be evaluated to ensure that they are not mistaken for changes of tectonic origin. Of these variables, precipitation appears to have the largest effect. For example, the drop in IBE of 15 min about 6 months before the Morgan Hill earthquake (Fig. 4C) is coincident with the largest 1-day value of precipitation of the year shown (above 9 cm). Closer examination of the data for the 6-month period before the Morgan Hill event reveals that daily rainfall above ~2.5 cm has often coincided with a nearly instantaneous (within a day) decrease in IBE (the rough response is a decrease of 2 min in IBE per centimeter of precipitation). The effect of precipitation can also be seen in the case of the Loma Prieta event. The largest 4-day period of precipitation of the year, commencing 5 days after the earthquake, is closely associated with the abrupt drop in IBE after the initial coseismic rise (Fig. 4D).

The most important question is whether precipitation could account for the signals we have attributed to tectonic causes. In the case of the Loma Prieta and Oroville events, this would be quite difficult because (i) there was no significant rainfall in the month preceding the Loma Prieta event or in the 3 months preceding the Oroville event and (ii) precipitation appears to induce interval shortening, not interval lengthening. The case of Morgan Hill is slightly less straightforward, because the IBE signal is a mode change, not interval lengthening. In addition, although there was no significant rainfall in the month before the earthquake (>2.5 cm), there were small amounts of precipitation (~1 cm) 4 and 8 days before the Morgan Hill event. Nevertheless, in consideration of the empirical evidence for an instantaneous IBE response to precipitation and the expected small change in IBE (1 to 2 min) from this rain, it is unlikely that precipitation produced the observed preseismic and coseismic changes in eruption mode.

Barometric pressure is a source of stress that plausibly could have an effect on the IBE. This notion was first considered by Rinehart (*11*) for Calistoga Geyser using IBE data from 1960 to 1969; he argued that there was a response on the time scale of a year. Most important for our purposes is the effect (of barometric pressure) on the scale of days to weeks; we see no evidence for such an effect. There are no unusually large excursions in pressure that could plausibly account for the coseismic or preseismic signals we have attributed to tectonic causes. This is illustrated for the case of the Loma Prieta earthquake (Fig. 5). There is, however, an observable indirect relation; an abrupt decrease in pressure often precedes precipitation, which, as we have seen, can produce a decrease in IBE. This is particularly clear in the case of the Loma Prieta and Morgan Hill earthquakes for the days of high precipitation mentioned above.

Two cultural activities that might have affected the IBE data are pumping in the town of Calistoga (3 km to the south) and production activity at The Geysers geothermal field (Fig. 1). Hydrological data suggest that it is unlikely for pumping in the town of Calistoga to have had a significant effect on the geyser (*19*). The Geysers geothermal field consists of 18 plants that convert steam into electrical power. It is apparently not connected hydrologically to Calistoga Geyser; nor is there evidence for a thermal connection (*19*). The available data do not suggest unusual changes in production coincidental with the times of the earthquakes under study.

A Test for Statistical Significance

What are the chances that the coseismic and preseismic signals are merely random fluctuations in the IBE? To answer this formally, we consider the coseismic and preseismic signals separately. For the coseismic case, we assume that the IBE is primarily sensitive to dynamic strain and identify N_e earthquakes that are as large as or larger than the three earthquakes appearing to have a geyser response, on the basis

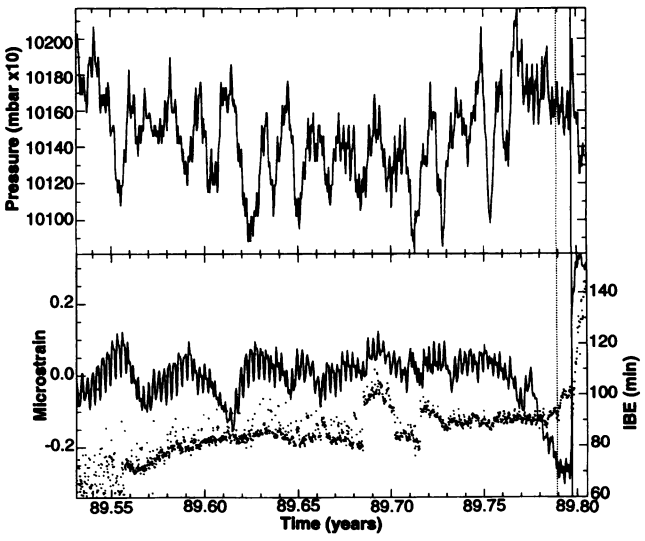

Fig. 5. Plot of 100 days before the Loma Prieta earthquake. (Bottom trace) Raw IBE data (same as Fig. 4A). (Middle trace) Extensometer recording from station PRE (Fig. 1). Direction: N73E. The positive direction corresponds to extension. Tides are the predominant periodic signal. The largest excursion in the record is the rapid drop beginning 7 days before the earthquake. The left vertical line marks the begin time of the proposed IBE precursor. (Top trace) Barometric pressure for the same time period (3-hour data from San Francisco, California).

calculated dynamic elastic strain (Fig. 2). In addition, we can estimate the number of geyser interval-lengthening events, $N_{g\ell}$, and geyser mode-changing events, N_{gm}, based on a careful examination of the entire interval T of the IBE record (1973 to 1991). An earthquake and geyser event are said to be coincident if the geyser event occurs within an interval ΔT of the earthquake occurrence. With $N_T = T/\Delta T$ intervals, we then take $p_\ell = N_{g\ell}/N_T$ and $p_m = N_{gm}/N_T$ as the probability of having one geyser event of each type occurring in any particular time interval. Then the combined probability P that two interval-lengthening events (P_ℓ) and one mode-changing event (P_m) are coincident with an earthquake is governed by the binomial distribution:

$$P = P_\ell P_m = \{[N_e - 1)/2]p_\ell^2(1 - p_\ell)^{N_e-2}\}$$
$$[N_e p_m(1 - p_m)^{N_e-1}]$$

Using $N_e = 8$ (from Fig. 2), $T = 6000$ days, $\Delta T = 6$ days (3 days before, 3 days after the earthquake), $N_{g\ell} = 10$, and $N_{gm} = 40$ (estimated number of IBE events comparable to the coseismic IBE variations for the three earthquakes), we find that $P \approx 7 \times 10^{-4}$ (*20*), so that the possibility of a coincidence is very small. We thus conclude that the coseismic geyser IBE variations are physically related to these three earthquakes.

For the preseismic case, what is the probability that the preseismic IBE variations associated with these same three earthquakes are due to chance alone? In this case we specify $N_e = 3$, $\Delta T = 3$ (3 days before the earthquake), $N_{g\ell} = 150$, and $N_{gm} = 40$ (estimated number of events comparable in size and character with preseismic IBE variations: specifically, the number of events with a 10- to 20-min increase in IBE, and the number of comparable mode changes, respectively). The probability is again very small, $P \approx 0.001$ (*21*). We thus reject the hypothesis that the coseismic or preseismic signals are due to random fluctuations in the IBE data.

Strain Data

In an attempt to corroborate the existence of one of the proposed precursors, we acquired and examined strain data available during and before the Loma Prieta earthquake. Data were obtained for stations PRE (tiltmeter, two extensometers) and BRK (tiltmeter), halfway between the earthquake and the geyser, and in addition for SRL (Sacks-Evertson dilatometer) (*3*) and MSJ (Gladwin tensor strainmeter) (*22*) south of the rupture zone (Fig. 1). A detrended extensometer recording at PRE (Fig. 5) shows an abrupt decrease (shortening) that began about 7 days before the earthquake. The excursion is roughly 0.3 microstrain and about three times tidal strains. It also has a time constant and form similar to that of the preseismic signal seen in the IBE data. The same signal was observed on both extensometers at PRE, eliminating instrumental artifact as a potential cause. The tiltmeters at PRE and BRK, however, did not show this same signal, although they are much less sensitive to horizontal shear, the most probable form of the precursory strain. The strainmeters south of the fault (SRL and MSJ) showed no obvious preseismic signal.

Precursor Characterization and Geyser Response

Taken at face value, the results suggest that at least some Northern California earthquakes exhibit observable precursory phenomena, a necessary prerequisite for successful earthquake prediction. Reports of such short-term precursory phenomena for large California earthquakes have been rare (*23*) with the notable exception of a magnetic field precursor to the Loma Prieta earthquake (*24*). Equally intriguing, the precursory changes were observed more than 130 km from the impending fault zone. This is hard to reconcile with the notion that precursors originate as preseismic slip on the fault. Although the coseismic dynamic strains for the three earthquakes studied are calculated to be quite large, about 10^{-6}, and probably account for the coseismic geyser response, the preseismic static strains would be expected to be much smaller (*6*), at most 10^{-8} to 10^{-9}. Because we have been unable to detect tidal strains (the O1 and M2 tidal lines) in the IBE data, corresponding to 10^{-8}, the strains caused by precursory slip on the fault would be far too small to account for the data. Values of at least 10^{-7} are probably required and would most likely be due to variations in regional strain that serve to load the impending fault zone. Directional loading of the Loma Prieta fault zone from the north, for example, could provide an explanation for the preseismic strain at station PRE (Fig. 5) of this order (about 3×10^{-7}), the presence of a signal at the geyser, and the absence of such signals at stations south of the fault. The existence of precursory changes in regional strain is suggested by other hydrologic data as well. Indeed, a recent worldwide compilation of precursory hydrologic phenomena shows that most observations beyond a distance of 150 km from the associated earthquake cannot be attributed to preseismic slip (*6*), and a mechanism such as regional strain is probably needed. In addition, a recent statistical approach to earthquake prediction (*25*) implies that large regions (several hundred kilometers) may be involved in the preparation phase of large seismic events.

The way in which the IBE responds to tectonic strain is not entirely known, although some plausible possibilities can be offered. The immediate reservoir of Calistoga Geyser extends to a depth of 70 m, is 30 cm in diameter (*16*), and is recharged by a deep high-temperature reservoir, within fractured volcanic rocks. Temporal variations in the IBE are probably controlled by changes in volumetric flow velocity Q associated with recharge (*18*). In this case, the closest analogy to the geyser would be the well draw-down problem for a confined aquifer. If we assume Darcy flow, Q is then proportional to $k\Delta H$, where k is permeability and ΔH is the difference in hydraulic head between the point of recharge (H_0) and the well (H_w). A drop in H_0 (increase in IBE) could result from microfracturing of the confining material and a partial draining of the aquifer. Such a mechanism has been proposed to account for the observed dramatic reduction in well levels (by as much as 20 m) and increased stream flow at a distance of 20 to 40 km from the Loma Prieta earthquake, presumably due to coseismic deformation (*26*). Alternatively, strain-induced changes in reservoir volume could produce significant changes in H_0 if the recharge zone is small compared to the size of the reservoir (for example, a narrow fault zone) (*27*). Finally, k could change through strain-induced variations in the size of preexisting microfractures within the reservoir. In hydrologic systems where fractures are nearly closed, large changes in permeability can occur with strains of the order 10^{-7} to 10^{-6} (*28*). Although we cannot at present choose between these mechanisms, they serve to illustrate the plausibility of a close relation between the IBE of an "old faithful–type" geyser and tectonic strain.

REFERENCES AND NOTES

1. H. Kanamori and J. J. Cipar, *Phys. Earth Planet. Inter.* **9**, 128 (1974).
2. I. Cifuentes and P. G. Silver, *J. Geophys. Res.* **94**, 643 (1989).
3. I. S. Sacks, S. Suyehiro, D. W. Evertson, Y. Yamagishi, *Pap. Meteorol. Geophys.* **22**, 195 (1971).
4. A. T. Linde, K. Suyehiro, S. Miura, I. S. Sacks, A. Takagi, *Nature* **334**, 513 (1988).
5. M. T. Gladwin, R. L. Gwyther, J. W. Higbie, R. Hart, *Geophys. Res. Lett.* **18**, 1377 (1991).
6. E. A. Roeloffs, *Pure. Appl. Geophys.* **126**, 177 (1988).
7. I. G. Kissin and A. O. Grinevsky, *Tectonophysics* **178**, 277 (1990).
8. P. G. Silver and N. J. Valette-Silver, *Nature* **326**, 589 (1987).
9. R. Hutchinson, *U.S. Geol. Surv. Open-File Rep. 85-290-A* (1985).
10. S. H. Wood, *ibid.*, p. 573.
11. J. Rinehart, *J. Geophys. Res.* **77**, 342 (1972).
12. E. T. Allen and A. L. Day, *Steam Wells and Other Thermal Activity at "The Geysers," California* (Publ. 378, Carnegie Institution of Washington, Washington, DC, 1927), p. 106.
13. R. S. Hart, R. Butler, H. Kanamori, *Bull. Seismol.*

Soc. Am. 67, 1 (1977).
14. H. Kanamori and K. Satake, *Geophys. Res. Lett.* 17, 1179 (1990).
15. The data for Fig. 3 have been passed through a median filter to enhance coherent features. A median filter is similar to the more familiar running mean filter, except that the median, rather than the mean, is used. Use of a median filter is preferred for time series with a large number of isolated outliers, which is the case for the geyser data. This filter preserves the sharpness of step-like changes in a time series. The sample length in Fig. 3 is 20 samples corresponding to between 15 and 30 hours. See W. H. Press, B. P. Flannery, S. A. Teukolsky, W. T. Vetterling, *Numerical Recipes* (Cambridge Univ. Press, Cambridge, 1986).
16. J. Rinehart, *Geysers and Geothermal Energy* (Springer-Verlag, New York, 1980).
17. S. W. Kieffer, *J. Volcanol. Geotherm. Res.* 22, 59 (1984).
18. S. W. Kieffer, *Rev. Geophys.* 27, 3 (1989).
19. D. Brock, personal communication.
20. The formula given is for the probability of exactly two interval-lengthening events and one mode-changing event being coincident with an earthquake, although the number quoted is for at least this number of coincidences.
21. The probability is most sensitive to the estimates of $N_{o\epsilon}$ and N_{gm}. It is unlikely, however, that we have underestimated these values by more than about 30%, which would increase the probability by no more than a factor of 3. One could argue that, for the preseismic case, it is more appropriate to consider N_e to be 5 rather than 3, on the basis of the number of events with comparable static strain (Fig. 2). Using this value increases P by a factor of 5. Allowing for both of these factors increases in probability, $P \sim 0.014$, which is still below the critical value for significance, taken here to be 0.05.
22. M. T. Gladwin, R. L. Gwyther, R. Hart, M. Francis, M. J. S. Johnston, *J. Geophys. Res.* 92, 7981 (1987).
23. K. Mogi, *Earthquake Prediction* (Academic Press, Tokyo, 1985).
24. A. C. Fraser-Smith *et al.*, *Geophys. Res. Lett.* 17, 1465 (1990).
25. V. I. Keilis-Borok, L. Knopoff, I. M. Rotwain, C. R. Allen, *Nature* 335, 690 (1988).
26. S. Rojstaczer, *Eos* 72, 121 (1991).
27. C. R. Carrigan, G. C. P. King, G. E. Barr, N. E. Bixler, *Geology* 19, 1157 (1991).
28. A. Nur, personal communication.
29. We thank O. Kolbek and the other workers at Calistoga Geyser, whose diligent monitoring of the geyser has made this study possible. We thank D. Power, who along with J. Dunlap and A. Sawyer entered more than 150,000 eruption times into the computer. E. Roeloffs, P. Rydelek, G. Helffrich, A. Linde, and I. Cifuentes provided reviews. We also thank A. Linde for numerous stimulating conversations as well as S. Sacks, S. Kieffer, D. White, S. Rojstaczer, S. Hickman, J. Rinehart, C. Carrigan, and D. Brock for helpful discussions. We thank M. Johnston for providing strain data. We thank M. Acierno for computer support and J. Dunlap for assistance with manuscript preparation. This research was sponsored by the Department of Terrestrial Magnetism, Carnegie Institution of Washington.

RESEARCH ARTICLE

Short-Lived Radioactivity and Magma Genesis

James Gill and Michel Condomines

Short-lived decay products of uranium and thorium have half-lives and chemistries sensitive to the processes and time scales of magma genesis, including partial melting in the mantle and magmatic differentiation in the crust. Radioactive disequilibrium between ^{238}U, ^{230}Th, and ^{226}Ra is widespread in volcanic rocks. These disequilibria and the isotopic composition of thorium depend especially on the extent and rate of melting as well as the presence and composition of vapor during melting. The duration of mantle melting may be several hundred millennia, whereas ascent times are a few decades to thousands of years. Differentiation of most magmas commonly occurs within a few millennia, but felsic ones can be tens of millennia old upon eruption.

Magmas form as the result of decompression of the mantle, advection of heat, or fluxing by fluids such as water. They originate by partial melting at grain boundaries and drain upward by permeable flow, eventually ascending in sheets or pipes. Afterward they evolve chemically (differentiate) when they stall, often in reservoirs in or near the base of the crust, through the precipitation of minerals (fractional crystallization) and exsolution of vapor in a closed system or through open-system processes such as mixing with other magmas or chemical exchange with the reservoir's surroundings (assimilation). We refer to these two processes as melting and differentiation, respectively, although in practice they may not be as separate in space or time as we implied above. Together they span the "age of magma," that is, the time between the beginning of partial melting and the eruption of this melt or its differentiate.

The types of magma as well as their processes and rates of formation vary in different tectonic settings. Buoyancy is primarily responsible for the separation of basaltic melt from matrix beneath large intraplate volcanoes such as Hawaii, whereas shear stress is more important at plate margin volcanoes at spreading centers and subduction zones (*1*). Some magmas must ascend through the crust at rates of a few centimeters per second, because they transport dense mantle xenoliths to the surface, whereas others have characteristics attributed to prolonged crustal interaction. Radioactive disequilibria are used to study three aspects of magma genesis: (i) the melting process, (ii) ascent and differentiation, and (iii) the source materials. We focus on ^{238}U-^{230}Th-^{226}Ra disequilibria and the $^{230}Th/^{232}Th$ tracer in volcanic rocks that have erupted during the last few millennia (*2–4*).

In addition to providing the heat that fuels convection and partial melting, the natural radioactive decays of U and Th produce short-lived nuclides that may provide quantitative measurements of trace element fractionation and porosity and of constraints on the temporal and spatial scale of magma formation. There are 41 intermediate decay products in the three U and Th decay chains, seven of which have been studied in magmatic systems (Table 1). These products and their parents include actinides (Th, U, Pa), an alkaline earth (Ra), a rare gas (Rn), and chalcophilic elements of low and variable volatility (Pb, Bi, Po). In addition, the behavior of U during magma genesis is sensitive to its oxidation state and fluid composition because its solubility in magmatic fluids increases with O fugacity (f_{O_2}) and the concentration of Cl or CO_3^{2-} in the fluids.

This topic is usually known as the study of U series disequilibrium (*5*). Secular radioactive equilibrium is reached when the numbers of atoms (N) of all nuclides in a decay series are inversely proportional to their decay constants (λ) so that their "activities" ($\lambda * N$) are equal. Equilibrium is reached after about five half-lives of the longest lived nuclide. Both melting and differentiation involve chemical reactions between solids, silicate or carbonate melts, and vapor composed of C, H, O, and halogens. These reactions fractionate many elements including those in the ^{238}U-^{206}Pb, ^{235}U-^{207}Pb, and ^{232}Th-^{208}Pb decay chains, resulting in disequilibrium (unequal activities) between nuclides in one or more of the decay series (Fig. 1). Trace element fractionations have long been used in the study of magma genesis processes. However, because radioactive equilibrium exists at the beginning of magma formation and is re-

J. Gill is with the Earth Sciences Department, University of California, Santa Cruz, CA. M. Condomines is at the Centre de Recherches Volcanologiques et URA 10 CNRS, Université Blaise Pascal, 63038 Clermont-Ferrand, France.